Electrical and Chemical Characterization of the Antioxidant Effects on Thermal Aging of Crosslinked Polyethylene (XLPE)

Simone Vincenzo Suraci, *Member, IEEE*, Anne Xu, Xavier Colin, and Davide Fabiani, *Senior Member, IEEE*

***Abstract*— This article presents a comprehensive study on the impact of antioxidants (AOs) on the aging process of insulating polymeric materials, specifically complex permittivity, conductivity, and ac breakdown (BD) voltage. Accelerated aging was achieved through high temperatures (up to 130 °C) in the air on crosslinked polyethylene (XLPE) both with and without AOs. In addition to electrical tests, chemical analyses were performed to better understand the role of AOs during thermal aging. The results indicate that AOs effectively inhibit oxidation, preventing the formation of degradation species. As long as AOs are present, minimal changes in the electrical properties are observed. However, once the AOs are almost completely depleted, oxidation products significantly alter the electrical properties, resulting in a worsening of the material electrical performance.**

***Index Terms*— Antioxidant, complex permittivity, conduction mechanisms, electric breakdown, polymer aging, space charge, thermal aging.**

I. Introduction

POLYMERS, being organic matter, may be subjected to aging phenomena, which cause the modification of their functional properties during their in-service life under the effects of chemical reagents combined with environmental and operational stresses, e.g., oxygen, water, temperature, radiation, and voltage.

There are multiple aging phenomena for polymeric materials, which are commonly classified into two categories: physical and chemical mechanisms [1]. Among the chemical aging mechanisms, oxidation is one of the most damaging [1]. While the study of oxidation in various polymers is well-documented in the literature [2], [3], [4], the research on its impact on electrical properties remains an ongoing topic. This is primarily due to the limited understanding of the relationship between the evolution of electrical properties and chemical changes [5], [6], [7], [8].

In general, the functional properties of polymers, including electrical ones, deteriorate due to oxidation. This is because oxygen is highly reactive with hydrocarbon groups, and its incorporation into the macromolecule under the form of polar products (in particular carbonyls and hydroxyls) significantly affects the polarity and conduction mechanisms of the polymer. As a result, it is found that the complex permittivity and electrical conductivity of the material increase [5], [6], [9].

In the field of chemistry, the literature widely deals with radical chain oxidation reactions, which is beyond the scope of this study [3]. However, it is crucial to emphasize that this type of reaction is thermally activated, and its chemical kinetics exhibit exponential behavior with temperature. Consequently, the appropriate operating temperature for electrical equipment must be carefully selected based on the specific application to avoid premature material failure. To delay or prevent the adverse effects of oxidation, special additives such as antioxidants (AOs) are commonly incorporated into the polymer matrix.

AOs are chemical compounds capable of inhibiting oxidation reactions. There are various types of AOs, and they may be used alone or in blend to create a synergistic effect and to guarantee longer resistance to oxidation.

Primary AOs, such as phenolic AOs and secondary aromatic amines, are radical scavengers. They donate their reactive hydrogen to the peroxy free radical to prevent the propagation step of the oxidation reaction.

Secondary AOs, such as thiodipropionates and phosphites, are hydroperoxide decomposers. They convert hydroperoxides, resulting from the stabilization by the primary antioxidant or the propagation step of the oxidation reaction, into non-radical species. Although AOs have a beneficial effect, they are polar molecules with therefore poor solubility in polyolefin matrices [10], [11] and a negative impact on complex permittivity and space charge properties [5], [12], [13]. For these two main reasons, their concentration is

Manuscript received 22 November 2023; revised 20 March 2024; accepted 28 May 2024. Date of publication 3 June 2024; date of current version 30 July 2024. This work was supported in part by the Euratom Research and Training Program 2014–2018 under Grant 755183 and in part by the National Recovery and Resilience Plan (NRRP) (Mission 04 Component 2 Investment 1.5–NextGenerationEU, Call for tender n. 3277 dated 30/12/2021) under Award 0001052 dated 23/06/2022. *(Corresponding author: Simone Vincenzo Suraci.)*

Simone Vincenzo Suraci and Davide Fabiani are with LIMES, Department of Electric, Electronic and Information Engineering, University of Bologna, 40126 Bologna, Italy (e-mail: simone.suraci@unibo.it; davide.fabiani@unibo.it).

Anne Xu is with the Saint-Gobain Recherche, 93300 Aubervilliers, France (e-mail: anne.xu@saint-gobain.com).

Xavier Colin is with PIMM, ENSAM, 75013 Paris, France (e-mail: xavier.colin@ensam.eu).

Color versions of one or more figures in this article are available at https://doi.org/10.1109/TDEI.2024.3408800.

Digital Object Identifier 10.1109/TDEI.2024.3408800

kept at a low level in polyolefin matrices, particularly for high-voltage applications, such as 0.3 wt.% for HVdc cable systems.

It is thus evident how the addition of AOs is, at the moment, the most reliable and easiest way to ensure the reaching of the design life of electrical equipment including all the types of cables (ranging from instrumentation and control to high-voltage ones). Despite various research articles focusing on the addition of micro- and nanofillers to enhance the insulation properties of power cables and capacitors [14], [15], [16], [17], [18], to the authors' knowledge, no work about the effect of the AOs on the evolution during aging of polymer electrical properties has been published yet.

The present work aims at: 1) providing a comprehensive view of the impact of AOs on the electrical properties of a base polymeric matrix and 2) highlighting how AO kinetics modify the electrical performances of these materials during thermal aging of the polymer. This is achieved by monitoring several key electrical properties of one of the most common insulating polymeric materials [crosslinked polyethylene (XLPE)] during accelerated thermal aging. This latter was conducted at temperatures between 87 °C and 130 °C in air. The chosen procedure ensures the reaction of added AOs with environmental oxygen, and it allows the investigation of the desired electrical properties throughout the entire aging process (from the antioxidants reactions and consumption to the inception of bulk oxidation). To provide consistency between the antioxidant kinetics and the state of the electrical properties, at each withdrawal time, the aged samples are first examined through chemical analyses. Then, the electrical properties are analyzed on the same samples, using both direct current (dc) and alternating current (ac) tests.

II. Materials and Methods

A. Materials and Aging

In this work, two material compounds are investigated, based on the same silane-XLPE (Si-XLPE) matrix. This material is widely used inside LV and MV cables due to its easy manufacturing and good properties. In addition to the pristine Si-XLPE (Compound #1), AOs were incorporated into the polymer matrix in the second compound to assess their impact on the investigated properties. The chosen primary antioxidant is a hindered phenol commonly referred to as Irganox[1] 1076, while the secondary antioxidant is the distearyl thiodipropionate of commercial reference Irganox PS802. The specifications and the structural chemical formulas of compounds are reported in Table I and Fig. 1, respectively.

Samples were provided by Nexans in the framework of the European Project H2020 TeaM Cables. The compounding procedure was performed according to the two-step Sioplas process [19]. During the first step, silane is grafted onto the polymer chain on twin screws and filled on a co-kneader. Then, the material is prepared into specimens in the form of plates and tapes. Plates were produced by compression molding (T higher than the melting point of PE) after blending the compounds with a catalyst on a twin-roll mixer. For tapes, the compounds and the catalyst are extruded together on the extrusion line with a rectangular-shaped head. Finally, obtained specimens are placed into water to initiate the cross-linking process.

[1]Registered trademark.

TABLE I
SPECIFICATIONS AND CHEMICAL COMPOSITION OF MATERIALS UNDER TEST

Compound index	Material composition		
	Si-XLPE matrix	Primary antioxidant	Secondary antioxidant
1	100 %wt	-	-
2	98 %wt	1 %wt	1 %wt

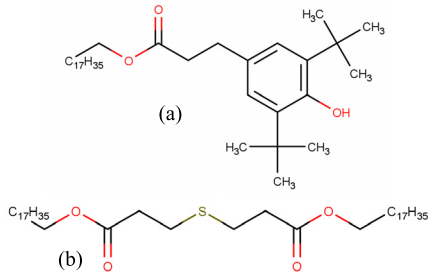

Fig. 1. Structural chemical formula of (a) Irganox 1076 and (b) IrganoxPS802.

TABLE II
ACCELERATED THERMAL AGING CONDITIONS

Withdrawal #	Aging durations		
	87 °C	110 °C	130 °C
1	3456 h	2592 h	2520 h
2	6912 h	5184 h	3456 h
3	10440 h	7776 h	5184 h
4	13824 h	10584 h	6912 h
5	17280 h	12960 h	8568 h

Tapes (4 × 4 cm) were used for chemical, dc conductivity, and permittivity measurements, while sheets (6 × 6 cm) were only used for ac breakdown (BD) tests. In both cases, the sample thickness of samples was ∼500 μm.

Before testing, specimens were degassed in the oven at 50 °C under a primary vacuum for at least 8 h, to remove any volatile product and absorb moisture.

Samples were subjected to accelerated thermal aging inside air-ventilated ovens. The chosen temperatures were: 87 °C, 110 °C, and 130 °C. The aging durations and the withdrawal times are reported in Table II. Note that, due to the enhanced degradation of pristine XLPE at the highest aging temperature (130 °C), it was not possible to perform tests for aging durations longer than ∼2600 h. For this reason, an additional aging campaign was performed at the same temperature with shorter and more frequent withdrawal times. Although the aged materials exhibited holes and extensive superficial damage (Fig. 2), they remained suitable for performing physical–chemical analyses after microsampling.

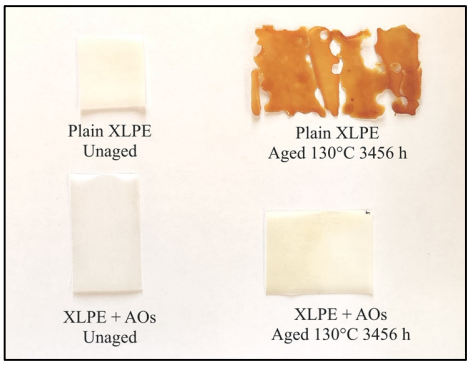

Fig. 2. Photograph of XLPE with and without AOs at equal aging conditions (after 3456 h at 130 °C). Top: pristine XLPE, Bottom: XLPE + AOs.

B. Chemical Characterization Tests

1) Oxidation Induction Time: Oxidation induction time (OIT) is a quantitative technique for the investigation of the antioxidant depletion kinetics in the insulation bulk. It records the time required to induce the oxidation reaction of the polymer matrix under pure O_2 flow in the molten state (typically $T \geq 190$ °C for polyolefins). After the running out of AOs, the oxidation reaction starts almost immediately causing the sudden appearance of an exothermic peak on the thermograph. The onset is determined graphically as the intersection point of the baseline with the steepest tangent of the increasing part of the exothermal peak (i.e., according to the so-called "tangent method").

OIT was measured with a TA instrument DSC Q10 calorimeter beforehand calibrated with an indium reference. The temperature for the isothermal step was set equal to 190 °C for compound #1 (pristine XLPE) and 210 °C for compound #2. The use of two different isothermal temperatures is needed to record appreciable variation during aging for pristine XLPE and to obtain results within an acceptable experimental time for compound #2. Samples (∼8 mg) were heated up in the furnace with a rate of 10 °C·min^{-1} under pure N_2 flow (50 mL·min^{-1}). After isothermal stabilization, gas in the furnace was switched to O_2. The test was considered complete after the entire detection of the exothermic peak assigned to the oxidation of XLPE.

2) Fourier Transform Infra-Red Spectroscopy: Fourier transform infra-red (FTIR) spectroscopy was used to detect the changes in the chemical composition of the insulation during aging (i.e., chemical consumption, migration, physical loss of AOs, and oxidation of XLPE). FTIR spectra were recorded through a PerkinElmer FTIR Frontier spectrometer equipped with a diamond/ZnSe crystal in attenuated total reflectance (ATR) mode. Each spectrum was averaged from 16 scans acquired in the spectral range 4000–650 cm^{-1}, with a resolution of 4 cm^{-1}.

To investigate the complex behavior of AOs before the arising of oxidation products in the XLPE matrix, mainly carboxyl acids, it was decided to refer to the carbonyl index (CI). For all aging durations, the most intense absorption band in the carbonyl region (typically between 1640 and 1880 cm^{-1}) was chosen for the calculation of CI

$$\text{Carbonyl index} = \frac{A_{\max\,(1700-1800\ \text{cm}^{-1})}}{A_{1472\ \text{cm}^{-1}}} \tag{1}$$

where $A_{\max\,(1700-1800\ \text{cm}^{-1})}$ is the absorbance of the most intense band in the carbonyl region, and $A_{1472\ \text{cm}^{-1}}$ is the absorbance of CH_2 scissoring vibration of the PE crystal phase at 1472 cm^{-1}, whose value is supposed not to change during aging (reference band).

Each specimen was tested at least three times to consider a possible inhomogeneous distribution of AOs and the formation of small spots typical of earlier localized oxidation.

C. Electrical Tests

1) DC Conductivity Measurements: DC conductivity was measured according to the ASTM D257-14 (2021) standard.

Before measurements, samples were properly metallized through plasma cold sputtering to define the electrode geometry. In particular, a grounded guard electrode was deposited on the material surface to get rid of the superficial current contribution to the registered current.

Current flowing through insulation was measured by means of a HVdc voltage generator (Keithley 2290E-5 5 kV) and a picoamperemeter (Keysight B2981A). The values were acquired until the steady-state regime was established (i_{cond}) or 24 h after the beginning of the test. The conductivity value was obtained as follows:

$$\sigma = \frac{J_c}{E} = \frac{i_{\text{cond}}/S}{E}(\text{S/m}) \tag{2}$$

where J_c is the current density (A/m^2), i_{cond} is the conduction current in the steady state regime (A), S is the sensing area (3.14 cm^2), and E is the electric field (set equal to 5 kV/mm in this work). The choice of this electric field possibly avoids the injection of additional charge carriers from the electrodes and ensures the derivation of material conductivity values in the Ohmic domain.

2) Space Charge Measurements (PEA Method): Space charge measurements were performed through the pulsed electro-acoustic (PEA) method [20].

In this work, the applied dc electric field was set equal to 10 kV/mm at room temperature, in a shielded environment. The choice of this electric field is compatible with the real applications of the Si-XLPE, as described in Section II-A. The volt-on phase lasted 10 000 s, while the volt-off phase lasted 3500 s.

Recall that the value of total absolute stored charge density in the bulk at a chosen depolarization time is given by [21]

$$q_s(E, t_d) = \frac{1}{1}\int_0^1 |q(x, E, t_d)|dx \tag{3}$$

where l is insulation thickness, t_d is the depolarization time, and $q(x, E, t_d)$ is the space charge profile detected at time t_d.

The maximum value of q_s, namely $Q_{\max}$, was calculated at the beginning of depolarization once the poling electrode charge had been dissipated, let's say at about $t_d = 5$ s.

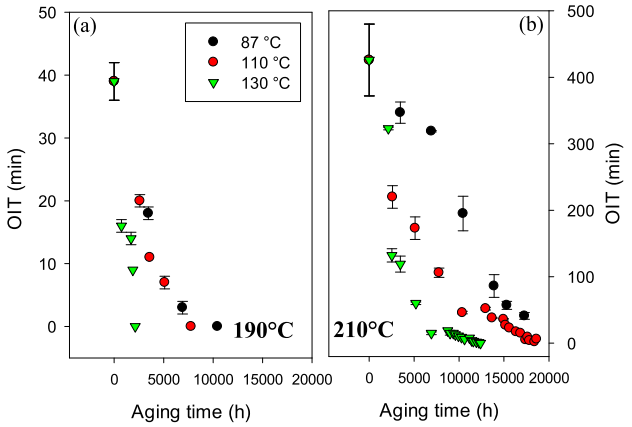

Fig. 3. OIT of the tested materials as a function of exposure time for various aging conditions. (a) Pristine XLPE (OIT measured at 190 °C). (b) XLPE + AOs (OIT measured at 210 °C).

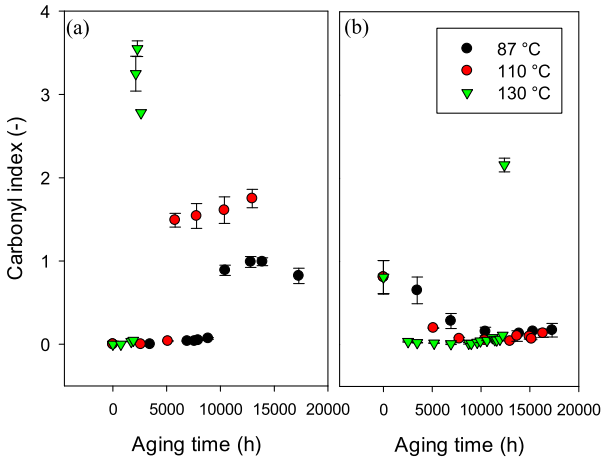

Fig. 4. Carbonyl index of the tested materials as a function of exposure time for various aging conditions. (a) Pristine XLPE. (b) XLPE + AOs.

3) Dielectric Spectroscopy Measurements: A Novocontrol Alpha Dielectric Analyzer v2.2 was used to investigate the complex permittivity trend as a function of the frequency of materials under test. The chosen frequency range extended from 0.1 Hz up to 1 MHz and tests were performed at 3 V_{rms}. Recall that the investigated frequency region allows the study of both dipolar and interfacial polarization phenomena [1]. For the sake of brevity, it was not possible to show the entire dielectric spectra of the materials under test. Thus, it was chosen to only report the values of complex permittivity (real and imaginary parts) as a function of aging for two fixed frequencies i.e., 0.1 Hz and 100 kHz. For information, the lowest frequency (0.1 Hz) is generally used in the standards (IEEE 400.2-2013) for tanδ measurements on electrical equipment (e.g., MV and HV cables). The highest frequency (100 kHz), in contrast, was reported in our previous works [6], [9] to be related to the aging evolution of polymeric materials, through the dipolar properties of degradation products (mainly polymeric oxidation products).

4) AC Breakdown Measurements: AC BD measurements were performed according to IEC EN 60243-1:2013 standard using a Baur DPA 75C oil tester.

The setup applies a ramp selected by the user which increases the 50 Hz ac voltage until the reaching of the BD. The chosen ramp was set equal to 1 kV/s to reach the breakdown voltage (BDV) within 30 s for all the sample benches. Samples were inserted between two sphere electrodes in a mineral oil bath to avoid discharge in the air. Measurements were performed in at least five points of the sample and experimental results were treated by means of Weibull analysis according to IEC 62539:2004 standard.

III. Results

A. Chemical Analysis Results

1) Oxidation Induction Time (OIT): With reference to the OIT values (Fig. 3), it is worth noting that the OIT scale of Fig. 3(b) is ten times larger than that of Fig. 3(a).

Although considering a pristine XLPE (no AO added during shaping), a small concentration of these additives is necessarily present in the polymer pellets to avoid premature oxidation during storage. For this reason, a nonzero, though low, value of OIT is seen in Fig. 3(a). Focusing on the trend, it can be seen that lower aging temperatures result in a slower decrease in the property, thus confirming that the oxidation reaction is thermo-activated. As a consequence, OIT vanishes at ∼2560, ∼7500 and ∼10 000 h for exposures at 130 °C, 110 °C and 87 °C, respectively. Therefore, it may be stated that for aging periods longer than the abovementioned durations, oxygen is free to react with XLPE chains to initiate oxidation.

As expected, AOs (compound #2) delay the oxidation reaction leading to higher values of OIT even at higher isothermal temperatures (210 °C). During aging, AOs are consumed and the protection against oxidation, assessed through OIT, is reduced. OIT does not vanish at the exposure temperatures of 110 °C and 87 °C, suggesting that a small concentration of AOs is still present in the XLPE matrix, even after the longest exposure period investigated in this work. It is therefore unlikely that oxidation was initiated in the context of the present study.

2) Carbonyl Index: The assessment of the carbonyl index may be considered as a complementary measurement technique to OIT. Ordinarily, if AOs are present, oxidation may not start and degradation products due to aging are limited or absent. They can only be degradation products of AOs. It has commonly been reported in the literature that the oxidation of XLPE leads to the formation of two main degradation products: hydroxyls and carbonyls [6], [22]. For this reason, an increase in the carbonyl index is expected.

Fig. 4 reports the trend of the carbonyl index as a function of exposure time for the different materials and aging conditions. The unaged pristine XLPE shows a starting CI value equal to zero. After a given time, which depends on the aging severity, the CI starts increasing due to the onset of oxidation. In particular, the increase in all properties, for all the aging conditions considered, is recorded once the OIT vanishes, which confirms the abovementioned explanation.

AOs by themselves are characterized by the presence of an ester group (see Fig. 1). For this reason, the unaged material

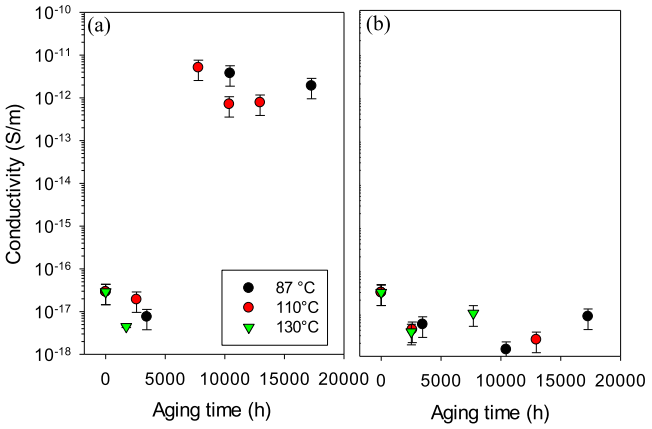

Fig. 5. DC conductivity of the tested materials as a function of exposure time for various aging conditions. (a) Pristine XLPE. (b) XLPE + AOs.

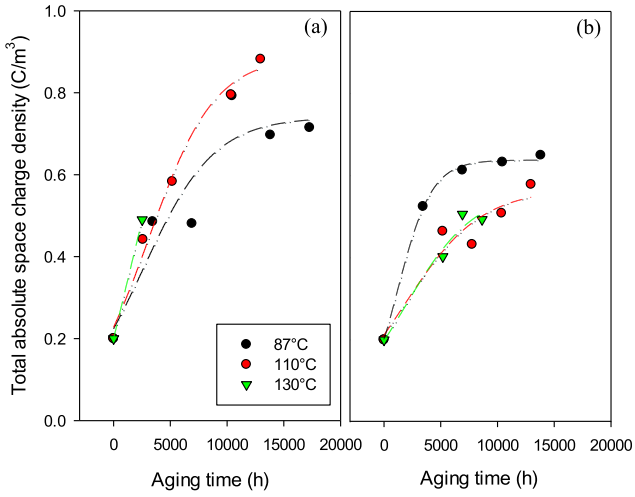

Fig. 6. Total absolute space charge density in tested materials as a function of exposure time for various aging conditions. (a) Pristine XLPE. (b) XLPE + AOs. Sigmoidal fitting.

(compound #2) shows a non-null CI value. During aging, AOs are consumed and converted into AO degradation products. As a consequence, the carbonyl index decreases to stay at a very low, almost constant value from the early periods of exposure. This suggests that no oxidation product arises during these first periods presumably due to the efficient protection of XLPE by AOs (OIT $>$ 0 min). Then, in the second stage, observable only for the longest duration (12 384 h) at the highest temperature of exposure (130 °C), CI re-increases suddenly and strongly due to the onset of XLPE oxidation.

Finally, it is worth noting that the final CI values are slightly higher at the lowest temperature of exposure (87 °C). A possible explanation would be that the physical loss of the degradation products of AOs would be slower at this temperature, which would allow their formation to be observed during aging.

B. Electrical Characterization

1) DC Conductivity: DC conductivity results for the tested materials are reported in Fig. 5. During the early periods of exposure, the value of conductivity is reduced for both compounds. Such a behavior has already been reported in the literature [23] and it is presumably attributed to the release of polar species such as crosslinking by-products and/or AOs.

With reference to compound #2 [Fig. 5(b)], the contribution of AOs to aging advancement is evident, keeping the conductivity values below 10^{-16} S/m for all the considered aging conditions.

On the contrary, in the absence of AOs [Fig. 5(a)], an initial decrease of the property (as for compound #2) followed by an abrupt increase by more than four orders of magnitude is observed. The inception time of this phenomenon is different depending on the aging conditions and as expected, occurs earlier in the case of aging at 110 °C (∼7500 h) in comparison to aging at 87 °C (∼10 000 h), as already seen with the chemical properties.

2) Space Charge Analyses: The total absolute space charge density as a function of exposure time for various aging conditions for the analyzed materials is reported in Fig. 6. As previously mentioned, the process of aging leads to the accumulation of degradation species, including oxidation products and radicals [3], [22]. These species can be viewed as deep traps that alter the conduction mechanisms within the studied polymer [12], [24], [25], [26]. Similarly, the total absolute space charge density (Fig. 5) and dc conductivity (Fig. 6) depict different trends between the two materials.

The pristine XLPE shows a continuous increase in the total absolute space charge density with exposure time until reaching an asymptotic value. As expected, higher temperatures (110 °C and 130 °C) show larger values of stored charges, thus indicating a stronger impact of aging stress.

The addition of AOs modifies the illustrated trend. In particular, the steepness of the curves does not follow the aging severity. On the contrary, the highest values are recorded for aging at 87 °C. Such a behavior is presumably imputable to the different AO degradation products arising at different temperatures, as already seen for CI. These new species may act as local traps, thus modifying the space charge density.

3) Dielectric Spectroscopy: The contribution of AOs to thermal aging is also evident by analyzing the trend of the complex permittivity (Fig. 7). As reported in Section II-C, it was chosen to report the experimental values for two fixed frequencies (100 kHz and 0.1 Hz) to evaluate the polarization mechanisms in terms of dipoles and interfaces, respectively.

The pristine XLPE shows a stepwise increase of the real part of permittivity up to 7 for both frequencies (Fig. 7(a) and (b)]. Here again, the aging temperature rules the inception time of the increasing trend (∼10 000 h for aging at 87 °C and ∼7500 h for aging at 110 °C).

The imaginary part of permittivity [Fig. 7(c) and (d)] exhibits a preliminary decrease at 100 kHz (dipolar polarization) presumably due to the consumption of polar species, as already discussed for the dc conductivity.

Then, the dielectric losses increase by more than one order of magnitude over exposure periods equal to those already reported for other electrical properties.

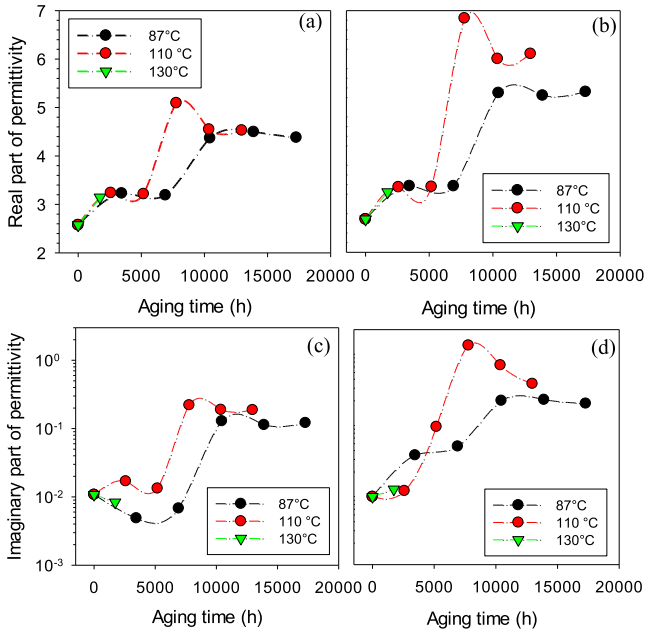

Fig. 7. Complex permittivity of pristine XLPE as a function of exposure time for various aging conditions. Real part of permittivity at (a) 100 kHz and (b) 0.1 Hz. Imaginary part of permittivity at (c) 100 kHz and (d) 0.1 Hz.

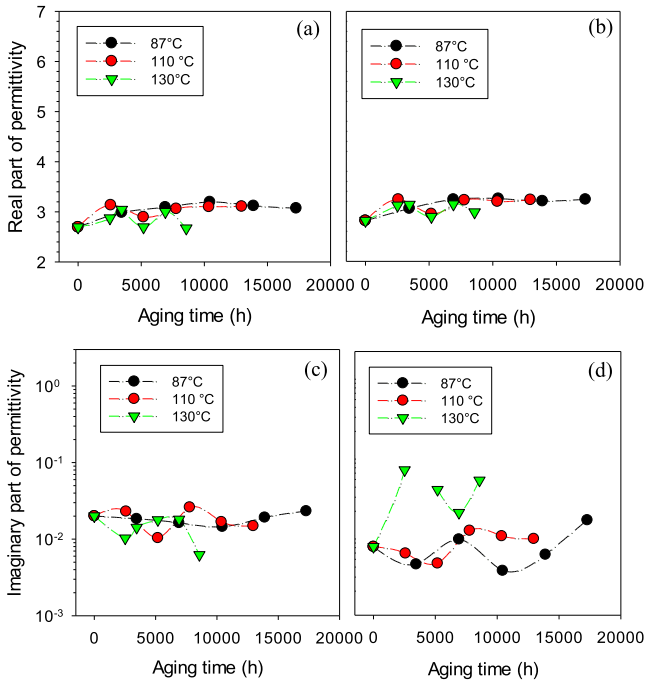

Fig. 8. Complex permittivity of XLPE with AOs as a function of exposure time for aging conditions. Real part of permittivity at (a) 100 kHz and (b) 0.1 Hz. Imaginary part of permittivity at (c) 100 kHz and (d) 0.1 Hz.

It is worth noting that the initial decrease is not observed for low frequencies (0.1 Hz). Two reasons can be considered. On the one hand, thermal aging modifies the interfacial microstructure, e.g., between crystalline and amorphous phases inside the polymer. On the other hand, the free ions species formed during aging may impact the low-frequency dielectric response, giving rise to conduction mechanisms.

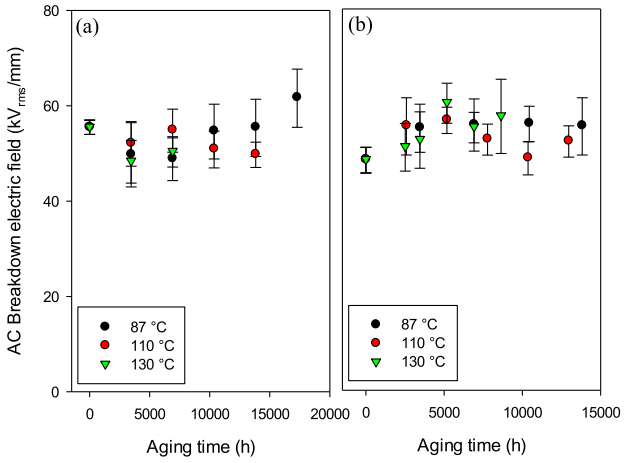

Fig. 9. 50 Hz ac Breakdown strength of tested materials as a function of exposure time for various aging conditions. (a) Pristine XLPE. (b) XLPE + AOs.

The introduction of AOs alters the trend described above. The real part of permittivity [Fig. 8(a) and (b)] is kept below the threshold value of ∼3 and little variation is measured during aging. The imaginary part of permittivity of the unaged material shows a slightly higher value than the pristine XLPE, likely due to the high polarity of AOs. During aging, the dielectric losses at 100 kHz kept an almost constant value, suggesting a limited increase of polar species. At 0.1 Hz, appreciable variations may be seen, particularly for the aging at 130 °C. Such behavior is imputable to interfacial rearrangements of crystals inside the polymer after annealing [27].

4) AC Breakdown Measurement Results: Fig. 9 reports the experimental data obtained for the 50 Hz dielectric strength test for the two materials. The unaged pristine XLPE exhibits a higher dielectric strength than XLPE with AOs. One explanation may be that the additives, located in the amorphous phase, may modify the local arrangement of the polymer chains, and cause the breakdown reduction.

During aging, the pristine XLPE shows a reduction of the breakdown strength. The values are then kept almost constant with wider data scatters. In particular, it is interesting to note that the exposure temperature seems not to impact the breakdown values.

For XLPE with AOs, the breakdown strength increases from the early periods of exposure (training effect). Then, it decreases to a level comparable to that of the unaged material.

IV. Discussion

The aging of polymeric materials with AOs may be summarized into three steps [5], [22].

1) Chemical consumption and physical loss of AOs.
2) Conversion of AOs into degradation species.
3) Oxidation of the polymer matrix.

In the case of crosslinked materials, the first aging phase may also be characterized by the release of crosslinking by-products. These chemical species are usually characterized by

high polarity and are found to act as deep traps in some polyolefin materials [12].

Normally, it is difficult to discern the two initial phases, since the physical consumption of OAs and their physical loss are very fast, and they occur during the early periods of exposure due to the high reactivity and mobility of AO molecules.

For the sake of this work, the discussion will be divided into three sections. The first two will highlight the contribution of each aging stage on the studied electrical properties, the latter will focus on the cross correlation between the different properties during oxidation.

A. Initial Consumption and Conversion of AOs

AOs have been shown to inhibit the oxidation and degradation of the polymer. In doing so, the short-term aging evolution may be considered as made up of multiple phenomena, i.e., the release of crosslinking by-products and chemical consumption and physical loss of AOs. Both may impact the electric properties of the material, these species being highly polar as seen in [12] and [25].

Regarding AO activity, during this stage, AOs may be lost physically, due to, e.g., evaporation, or be chemically converted into AO degradation products. In this case, AOs react with radicals and hydroperoxides forming new products such as cinnamate in the case of Irganox 1076 [11], [28]. Such a product contains the same ester and phenol groups as the starting AO. Hence, similar polarity properties are expected between the two species.

In the case of XLPE with AOs (compound #2), AO molecules are still present for the longest period of exposure considered in this work, as confirmed by non-null OIT values [Fig. 3(b)]. Thus, not all the AO molecules are converted, and the polarity of the material may be considered almost invariant during aging. Minor variations in terms of dipolar polarization (100 kHz) [Fig. 8(c)] during the early periods of periods are likely to be attributable to the release of crosslinking by-products.

During this stage, other electrical properties, such as electric conductivity and space charge characteristics, are affected. In particular, as seen in Fig. 5, the conductivity value decreases by almost one order of magnitude during the first periods of exposure. In addition to the removal of crosslinking by-products, newly formed species (e.g., AO degradation products) would be responsible for lower conduction properties.

These species may act as trap centers leading to the increase of the total absolute space charge density [Fig. 6(b)]. In particular, either bigger numbers or deeper traps are produced by reactions involving AOs. With reference to the CI of compound #2 [Fig. 4(b)], it may be noticed that the aging at 87 °C shows the highest values in terms of carbonyl species, suggesting a higher number of trap sites than in the other two cases. An additional reason for this result may be related to the different activities of AOs with temperature. Recall that AOs are characterized by an optimal operating temperature range. In this interval (∼100 °C as in various AOs), the conversion of AOs is more efficient, hence the number of trap sites may be reduced.

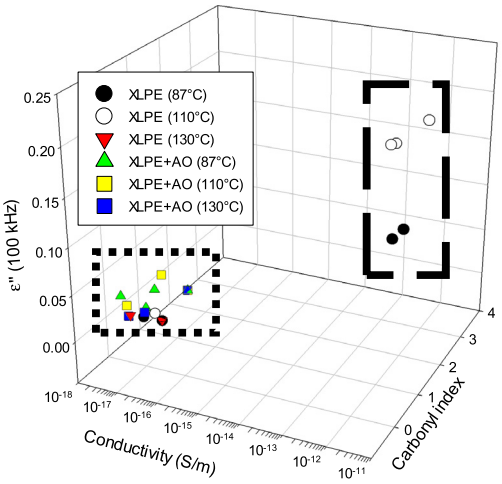

Fig. 10. Conductivity and dielectric losses as a function of carbonyl index. Dotted and dashed data cluster refers to unoxidized and oxidized materials, respectively.

B. Oxidation of the Polymer

After the complete consumption of antioxidants, oxygen can easily react with the hydrocarbon groups of the polymer, leading to chain scissions and giving birth to a wide variety of oxidation products, i.e., ketones, aldehydes, carboxylic acids, alcohols, etc.

These latter are widely reported in the literature to impact the electrical properties [6] due to their high polarity, high trap depth, and usually high conductivity. Indeed, oxidation products lead to the worsening of all the electrical properties studied in this work, except for ac breakdown [Fig. 9(a)].

The increase in carbonyl index [Fig. 4(a)] starts at different times depending on the severity of aging (∼10 000 h for 87 °C, ∼7500 h for 110 °C and ∼2500 h for 130 °C).

These induction times also correspond to the onset of the most marked variations in electrical properties, confirming the intimate relationship between the formation of oxidation products and the loss of electrical performance. In this sense, it would be possible to correlate the worsening of some electrical properties with the progress of oxidation. This correlation is highlighted through the 3-D graph relating the values of some electrical properties with the carbonyl index (Fig. 10). In this figure, it is possible to recognize two data clusters related to unoxidized and oxidized materials, respectively.

C. Electrical Properties at Oxidation Onset

It is worth recalling that the temperature dependence of the oxidation kinetics obeys an exponential law, as seen, e.g., in [4] and [29]. For this reason, the induction time of oxidation may be considered as an alarming point beyond which the material properties are expected to worsen very fast, and a serious condition monitoring or maintenance of the electrical equipment needs to be performed. For this reason, induction

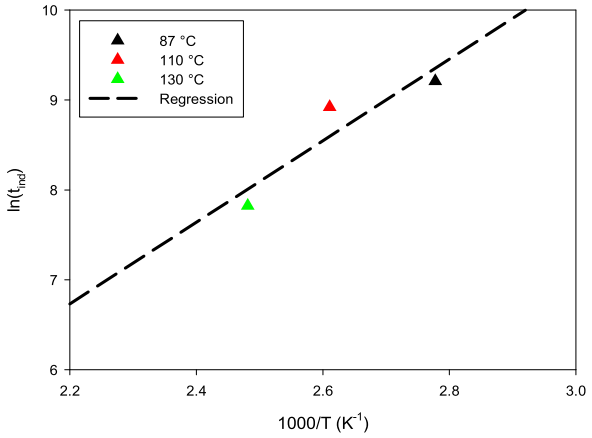

Fig. 11. Arrhenius plot of the oxidation induction.

TABLE III
VALUES OF THE ELECTRICAL PROPERTIES AT THE ONSET OF OXIDATION

	Aging condition		
	87 °C	110 °C	130°C
Induction time (h)	~ 10,000 h	~ 7,500 h	~ 2,500 h
	Electrical properties		
σ (S/m)	~ 5 × 10^{-11}	~ 5 × 10^{-11}	N/A
ρ (C/m^3)	~ 0.6	~ 0.6	N/A
ε' (-)	~ 4.2 (100 kHz) ~ 5.2 (0.1 Hz)	~ 4.5 (100 kHz) ~ 7 (0.1 Hz)	N/A
ε'' (·10^{-1})	~ 1 (100 kHz) ~ 2 (0.1 Hz)	~ 2 (100 kHz) ~ 20 (0.1 Hz)	N/A

times of oxidation (t_{ind}) may be suitable for insulation lifeline evaluation whose behavior is described by the well-known Arrhenius equation [30]

$$\ln(t_{ind}) = \ln(A) + E_a/kT \quad (4)$$

where A is a parameter dependent on the insulation characteristics and failure mode, E_a is the activation energy of the oxidation process (eV), k is Boltzmann's constant (eV/K), and T is the aging temperature (K). By introducing the OIT values in (4), we obtain A and E_a equal to 0.04 and 0.39 eV, respectively. Arrhenius plot is reported in Fig. 11.

Table III reports the values of the studied electrical properties at the onset of oxidation, as seen from the CI (Fig. 4).

In general, these values indicate a poor insulation system, restricting its potential applications to low-power electrical equipment. As an example, the properties from the table may be inappropriate for HV applications also at rated conditions such as the conductivity and the dielectric losses are extremely high, possibly leading to premature system failure, e.g., breakdown due to thermal instability. On the other hand, values in Table III may be still acceptable for other applications, i.e., LV electronics and cables where the electrical stresses may give a limited contribution to aging. In this case, as seen in our previous works [22], the primary cause of material failure is related to the poor mechanical properties, which deplete at a faster pace than other properties during aging. Furthermore, from Table III it is possible to notice how the values are equal (or sufficiently similar) among the different aging conditions, suggesting the possibility of defining reference values per each electric property. This result is of particular interest since the electrical measurements are non-destructive and they may be proposed as suitable condition monitoring techniques for electrical equipment, ensuring its correct operation and maintenance planning.

With reference to the complex permittivity, choosing the appropriate frequency may be an important discerning factor. Unlike the case at 0.1 Hz, the results at 100 kHz (dipolar polarization) are quite similar among the different aging conditions. In the framework of the desired derivation of reference values, the choice of this frequency is also suggested with reference to its ability to track aging, as reported in previous literature [5], [9].

V. CONCLUSION

In this article, a comprehensive analysis of the effect of AOs on the thermal aging of XLPE materials has been presented and discussed.

The tested materials highlighted the effectiveness of AOs in preventing degradation reactions, thus guaranteeing good insulating properties throughout the accelerated aging process studied in this work. In particular, the following conclusions may be drawn.

1) During the early periods of exposure, a general improvement of the electrical properties (e.g., reduction of electric conductivity and dielectric losses) is shown. This behavior was likely imputed to the chemical consumption and physical loss of AOs, and the release of crosslinking by-products.
2) The onset of oxidation, as confirmed by the increase of carbonyl index, leads to the worsening, up to numerous orders of magnitude, of the electrical properties, i.e., increase of complex permittivity, electrical conductivity, and accumulated charge.
3) Antioxidant reactions with radicals and hydroperoxides create new species (antioxidant degradation products) which tend to reduce the electrical conductivity, but they increase the total absolute space charge density presumably due to the arising of deeper traps.
4) Complex permittivity is shown to be kept to values similar to the unaged sample as long as AOs are present. Further aging results in an increase in the property, similar to additive-free XLPE.
5) AC breakdown strength is found to be almost invariant for the exposure conditions investigated in this work, exhibiting variations up to a maximum of 10% compared to the reference value.

Finally, it is demonstrated that the values of the electrical properties corresponding to the onset of oxidation are similar for the different exposure conditions. In the framework of the use of electrical measurements as condition monitoring techniques for electrical equipment, this study provides reference values that may be considered as warning values

beyond which the maintenance of the considered electrical equipment is needed.

Future work on this topic will include further analyses on the oxidation level throughout the polymer thickness through, i.e., microindentation and microscope-assisted FTIR, to highlight the possible effect of inhomogeneous oxidation on electrical properties.

REFERENCES

[1] J. D. Menczel and R. B. Prime, *Thermal Analysis of Polymers*. Hoboken, NJ, USA: Wiley, 2009, doi: 10.1002/9780470423837.

[2] X. Colin, "Humid and thermal oxidative ageing of radiation cured polymers—A brief overview," *Frontiers Chem.*, vol. 9, Jan. 2022, Art. no. 797335, doi: 10.3389/fchem.2021.797335.

[3] B. Fayolle, E. Richaud, X. Colin, and J. Verdu, "Review: Degradation-induced embrittlement in semi-crystalline polymers having their amorphous phase in rubbery state," *J. Mater. Sci.*, vol. 43, no. 22, pp. 6999–7012, Nov. 2008, doi: 10.1007/s10853-008-3005-3.

[4] M. C. Celina, "Review of polymer oxidation and its relationship with materials performance and lifetime prediction," *Polym. Degradation Stability*, vol. 98, no. 12, pp. 2419–2429, Dec. 2013, doi: 10.1016/j.polymdegradstab.2013.06.024.

[5] S. V. Suraci, D. Fabiani, S. Roland, and X. Colin, "Multi scale aging assessment of low-voltage cables subjected to radio-chemical aging: Towards an electrical diagnostic technique," *Polym. Test.*, vol. 103, Nov. 2021, Art. no. 107352, doi: 10.1016/j.polymertesting.2021.107352.

[6] S. V. Suraci, X. Colin, and D. Fabiani, "Multiscale modeling of permittivity of polymers with aging: Analysis of molecular scale properties and their impact on electrical permittivity," *IEEE Trans. Dielectr. Electr. Insul.*, vol. 29, no. 5, pp. 1795–1802, Oct. 2022, doi: 10.1109/TDEI.2022.3193869.

[7] S. Hettal, S. V. Suraci, S. Roland, D. Fabiani, and X. Colin, "Towards a kinetic modeling of the changes in the electrical properties of cable insulation during radio-thermal ageing in nuclear power plants. Application to silane-crosslinked polyethylene," *Polymers*, vol. 13, no. 24, p. 4427, Dec. 2021, doi: 10.3390/polym13244427.

[8] Y. Ohki and N. Hirai, "Thermal ageing of soft and hard epoxy resins," *High Voltage*, vol. 8, no. 1, pp. 12–20, Feb. 2023, doi: 10.1049/hve2.12259.

[9] E. Linde, L. Verardi, D. Fabiani, and U. W. Gedde, "Dielectric spectroscopy as a condition monitoring technique for cable insulation based on crosslinked polyethylene," *Polym. Test.*, vol. 44, pp. 135–142, Jul. 2015, doi: 10.1016/j.polymertesting.2015.04.004.

[10] A. Xu, S. Roland, and X. Colin, "Physico-chemical characterization of the blooming of Irganox 1076® antioxidant onto the surface of a silane-crosslinked polyethylene," *Polym. Degradation Stability*, vol. 171, Jan. 2020, Art. no. 109046, doi: 10.1016/j.polymdegradstab.2019.109046.

[11] E. Blázquez-Blázquez, M. L. Cerrada, R. Benavente, and E. Pérez, "Identification of additives in polypropylene and their degradation under solar exposure studied by gas chromatography–mass spectrometry," *ACS Omega*, vol. 5, no. 16, pp. 9055–9063, Apr. 2020, doi: 10.1021/acsomega.9b03058.

[12] S. V. Suraci, D. Mariani, and D. Fabiani, "Impact of antioxidants on DC and AC electrical properties of XLPE-based insulation systems," *IEEE Access*, vol. 11, pp. 76132–76141, 2023, doi: 10.1109/access.2023.3297495.

[13] S. V. Suraci, D. Fabiani, and C. Li, "Additive effect on dielectric spectra of crosslinked polyethylene (XLPE) used in nuclear power plants," in *Proc. IEEE Electr. Insul. Conf. (EIC)*, Jun. 2019, pp. 410–413, doi: 10.1109/EIC43217.2019.9046600.

[14] H. Zhang, Y. Duan, M. Xie, G. Ma, P. Li, and J. Qin, "The effects of TiO_2 nanoparticles on the temperature-dependent electrical and dielectric properties of polypropylene," *Frontiers Energy Res.*, vol. 10, pp. 1–11, Sep. 2022.

[15] T. Andritsch, A. Vaughan, and G. C. Stevens, "Novel insulation materials for high voltage cable systems," *IEEE Elect. Insul. Mag.*, vol. 33, no. 4, pp. 27–33, Jul. 2017, doi: 10.1109/MEI.2017.7956630.

[16] V. Tomer, G. Polizos, C. A. Randall, and E. Manias, "Polyethylene nanocomposite dielectrics: Implications of nanofiller orientation on high field properties and energy storage," *J. Appl. Phys.*, vol. 109, no. 7, Apr. 2011, Art. no. 074113, doi: 10.1063/1.3569696.

[17] O. G. Gnonhoue, A. Velazquez-Salazar, É. David, and I. Preda, "Review of technologies and materials used in high-voltage film capacitors," *Polymers*, vol. 13, no. 5, p. 766, Feb. 2021, doi: 10.3390/polym13050766.

[18] I. Rytöluoto et al., "Biaxially oriented silica–polypropylene nanocomposites for HVDC film capacitors: Morphology-dielectric property relationships, and critical evaluation of the current progress and limitations," *J. Mater. Chem. A*, vol. 10, no. 6, pp. 3025–3043, 2022, doi: 10.1039/d1ta10336a.

[19] *The Sioplas Process*, Midland Silicones, Michigan, 1968.

[20] G. C. Montanari, P. Seri, M. Ritamäki, K. Lahti, I. Rytöluoto, and M. Paajanen, "Performance of nanoparticles in the electrical behavior of DC capacitor films," in *Proc. 12th Int. Conf. Properties Appl. Dielectric Mater. (ICPADM)*, May 2018, pp. 41–44, doi: 10.1109/ICPADM.2018.8401024.

[21] G. Mazzanti, G. C. Montanari, and J. M. Alison, "A space-charge based method for the estimation of apparent mobility and trap depth as markers for insulation degradation-theoretical basis and experimental validation," *IEEE Trans. Dielectr. Electr. Insul.*, vol. 10, no. 2, pp. 187–197, Apr. 2003, doi: 10.1109/TDEI.2003.1194099.

[22] S. Hettal, S. Roland, K. Sipila, H. Joki, and X. Colin, "A new analytical model for predicting the radio-thermal oxidation kinetics and the lifetime of electric cable insulation in nuclear power plants. Application to silane cross-linked polyethylene," *Polym. Degradation Stability*, vol. 185, Mar. 2021, Art. no. 109492, doi: 10.1016/j.polymdegradstab.2021.109492.

[23] J. Cenes et al., "Assessment of the impact of the electrical stress on the ageing for a HVDC model cable," presented at the 10th Int. Conf. Insulated Power Cables, Versailles, Paris, 2019, pp. 1–6.

[24] M. Unge, C. Törnkvist, and T. Christen, "Space charges and deep traps in polyethylene—Ab initio simulations of chemical impurities and defects," in *Proc. IEEE Int. Conf. Solid Dielectr. (ICSD)*, Jun. 2013, pp. 935–939, doi: 10.1109/ICSD.2013.6619874.

[25] M. Meunier, N. Quirke, and A. Aslanides, "Molecular modeling of electron traps in polymer insulators: Chemical defects and impurities," *J. Chem. Phys.*, vol. 115, no. 6, pp. 2876–2881, Aug. 2001, doi: 10.1063/1.1385160.

[26] S. V. Suraci, C. Spinazzola, and D. Fabiani, "Analysis on the impact of additives on space charge behavior of thermally aged XLPE plaques," in *Proc. IEEE Conf. Electr. Insul. Dielectric Phenomena (CEIDP)*, Oct. 2022, pp. 41–44.

[27] M. Samet, A. Kallel, and A. Serghei, "Polymer bilayers with enhanced dielectric permittivity and low dielectric losses by Maxwell–Wagner–Sillars interfacial polarization: Characteristic frequencies and scaling laws," *J. Appl. Polym. Sci.*, vol. 136, no. 22, p. 47551, Jun. 2019, doi: 10.1002/app.47551.

[28] A. Xu, S. Roland, and X. Colin, "Physico-chemical analysis of a silane-grafted polyethylene stabilised with an excess of Irganox 1076®. Proposal of a microstructural model," *Polym. Degradation Stability*, vol. 183, Jan. 2021, Art. no. 109453, doi: 10.1016/j.polymdegradstab.2020.109453.

[29] M. Celina, E. Linde, D. Brunson, A. Quintana, and N. Giron, "Overview of accelerated aging and polymer degradation kinetics for combined radiation-thermal environments," *Polym. Degradation Stability*, vol. 166, pp. 353–378, Aug. 2019, doi: 10.1016/j.polymdegradstab.2019.06.007.

[30] H.-G. Lee, J.-S. Jung, and J.-G. Kim, "Measurement of activation energy and accelerated degradation time by thermal analysis methods for polymeric insulating materials," *J. Electr. Eng. Technol.*, vol. 16, no. 1, pp. 515–524, Jan. 2021, doi: 10.1007/s42835-020-00606-3.

Open Access funding provided by 'Alma Mater Studiorum - Università di Bologna' within the CRUI CARE Agreement